ELSEVIER

Journal of Alloys and Compounds 317–318 (2001) 13–18

Journal of ALLOYS AND COMPOUNDS

www.elsevier.com/locate/jallcom

Theoretical investigation of $L1_0$-disorder phase equilibria in Fe–Pd alloy system

T. Mohri[a,*], T. Horiuchi[b], H. Uzawa[a], M. Ibaragi[a], M. Igarashi[b], F. Abe[b]

[a]*Division of Materials Science and Engineering, Graduate School of Engineering, Hokkaido University, Sapporo 060-8628, Japan*
[b]*Frontier Research Center for Structural Materials, National Research Institute for Metals, 1-2-1 Sengen, Tsukuba, Ibaraki 305-0047, Japan*

Abstract

Lennard-Jones type pair-interaction energies are derived for Fe–Fe, Fe–Pd and Pd–Pd nearest neighbor pairs based on the thermodynamic data of cohesive energies, heats of formation and lattice constants. The dependency on the atomic separation is incorporated in each interaction energy. The configurational entropy is formulated within the tetrahedron approximation of the Cluster variation method by explicitly taking the tetragonality into account. Then, the free energy of the system is formulated as a function of cluster probabilities up to a tetrahedron cluster, nearest neighbor atomic separations and the tetragonality. Experimental transition temperatures of $L1_0$-disorder are reproduced accurately by incorporating the tetragonal distortion, and a preliminary analysis suggests that the additional magnetic interaction leads to a stabilization of the $L1_0$ ordered phase.

Keywords: Cluster variation method; $L1_0$ ordered phase; Lennard-Jones type potential; Fe–Pd phase equilibria

1. Introduction

Precipitation strengthening by the ordered phase $L1_0$ in the Fe–Pd system has been attracting broad attention [1]. Yet, the theoretical investigation of phase equilibria is not sufficient to provide useful information for the design of alloys. In view of the fact that the mechanical properties are largely influenced by atomic configuration of the ordered phase, it is desirable to employ a theory that is capable of providing detailed information on a discrete lattice. This study is motivated by such a requirement, and the main focus is placed on modeling the $L1_0$-disorder phase equilibria with an emphasis on calculating a phase diagram.

Theoretical calculations of phase equilibria have been advanced based on various methods. Among them, the Cluster variation method (hereafter CVM) [2] has been recognized as one of the most reliable tools. The advantage of the CVM is that the wide range of atomic correlations, which play an essential role in order–disorder transformations, are properly incorporated in the free energy formula. Therefore, accurate determinations of both transformation temperature and phase boundaries are expected.

The atomic interaction energies play a crucial role in determining stable phases. Although the elaborate first-principles calculation is desirable to derive interaction energies, this study is limited to empirical pair-wise interaction energies within Lennard-Jones-type interactions (hereafter L-J potential). In fact, the combination of L-J potential with the CVM [3–5], to calculate a phase diagram, has been successfully developed for various alloy systems and the scheme has been accepted as being one with reliable phenomenological methods. However, the incorporation of tetragonality, which is the essential feature of most $L1_0$ ordered phases, has not been attempted very much as yet, in particular for the present Fe–Pd system.

When a constituent element is a magnetic element, as in the case of Fe, the magnetic interactions may affect the location of phase boundaries. Unlike the case of chemical interaction energies, not many studies have been performed on the effects of magnetism. In this report, preliminary studies attempted to incorporate the combined effects of chemical and magnetic interactions within the framework of cluster variation free energy.

The organization of this report is as follows. In the next section, L-J type atomic interaction energies are introduced and the ground state analysis is attempted. An outline of the CVM is described in the third section, and the free energy of the present model is introduced. In the final section, calculated phase diagrams are demonstrated, and a

*Corresponding author.

0925-8388/01/$ – see front matter
PII: S0925-8388(00)01408-0

particular emphasis of the discussion is placed on the effects of magnetism.

2. Lennard-Jones potential and the cluster variation method

As shown in Fig. 1, the $L1_0$ ordered phase is well characterized as a layered structure along a [001] direction with alternative successions of (001) planes occupied by either *A* or *B* atoms. The lattice site preferentially occupied by an *A(B)* atom is termed the α(β) sublattice point. In most $L1_0$ ordered phases, the *a* and *c* axes differ in magnitude, inducing the tetragonal distortion that is characterized by the c/a ratio (hereafter θ). For a stoichiometric FePd–$L1_0$ ordered compound, a slight tetragonal distortion was also confirmed and the reported value of θ is ~0.96 [6,7].

As was mentioned in the previous section, the atomic interaction energy is described within the Lennard-Jones-type pair-wise potential, written as

$$e_{ij}(r) = e_{ij}^0 \cdot \left\{ \left(\frac{r_{ij}}{r}\right)^m - \frac{m}{n} \cdot \left(\frac{r_{ij}}{r}\right)^n \right\} \quad (1)$$

where e_{ij}^0, r_{ij}, m and n are Lennard-Jones' parameters. Among them, it has been well accepted that $m=7.0$ and $n=3.5$ describe a metallic alloy system quite well. The other parameters are determined by experimental data of cohesive energies [8,9] and lattice constants of Fe [10,11] and Pd [10,12], heats of formation [8,9,13] and lattice constants [7] of FePd with an $L1_0$ structure. The procedure was originally proposed for the investigation of γ/γ' phase equilibrium in a Ni–Al system [3] and, since then, various successful calculations have been performed. In a strict sense, data on cohesive and formation energies and lattice constants should be data obtained at 0 K, whereas available experimental data are mostly at finite temperatures and, therefore, extrapolation to 0 K is indispensable. In the present calculations, we also took the allotropic transformations involved in pure Fe into account when e_{FeFe}^0 was determined. The detailed procedure used to determine the L-J potential will be reported elsewhere [14]. In Tables 1 and 2, respectively, we provide the derived L-J parameters and the thermodynamic and structural data used. The resultant pair interaction energies are shown in Fig. 2. One can see that e_{FePd} is the deepest, indicating the ordering tendency of the system.

With atomic interaction energies, the internal energy per lattice point is given as

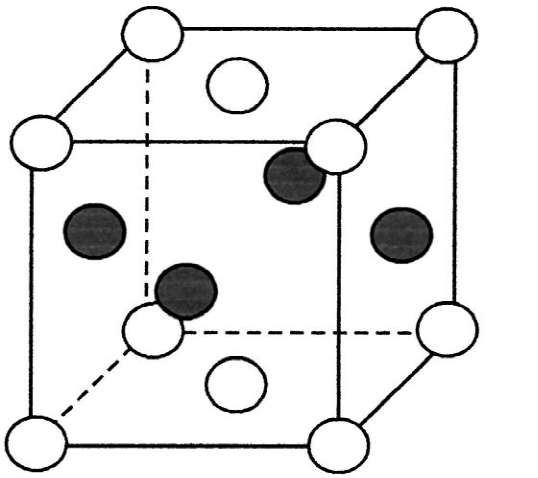

Fig. 1. Atomic configuration of the $L1_0$ ordered structure. Open and solid circles indicate *A* and *B* atoms, respectively.

Table 1
Lennard-Jones parameters determined for the three kinds of pairs

	e_{ij}^0 (kcal/mol)	r_{ij} (Å)
Fe–Fe pair	16.15	2.517
Pd–Pd pair	15.00	2.744
Fe–Pd pair	17.04	2.710

Table 2
Employed thermodynamic and structural data in determining the Lennard-Jones parameters in Table 1

	Lattice constant (Å)	Cohesive energy/heat of formation (kcal/mol)
Pure Fe (fcc)	3.559	−96.9
Pure Pd	3.880	−90.0
Fe–Pd $L1_0$	*a*, 3.855; *c*, 3.714	−98.5

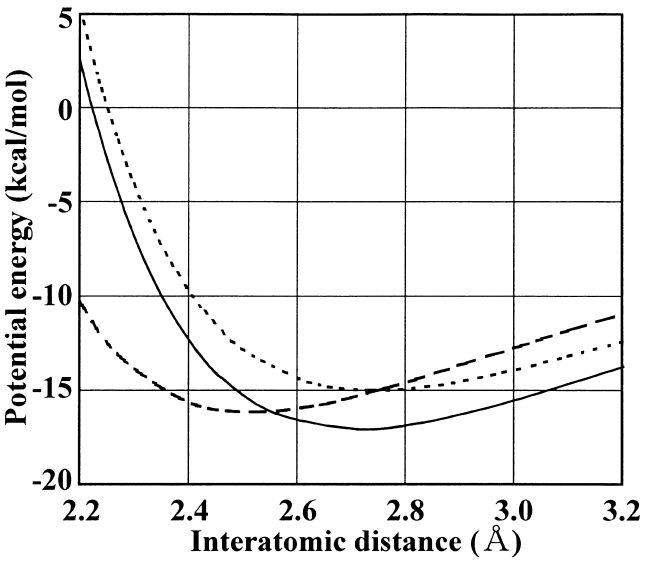

Fig. 2. Derived Lennard-Jones potentials for the Fe–Pd system. The broken, solid and dotted lines indicate the potentials for Fe–Fe, Fe–Pd and Pd–Pd, respectively.

$$E(\{r^{\gamma\delta}\}) = \sum_{\gamma,\delta} \omega^{\gamma\delta} \sum_{i,j} e_{ij}(r^{\gamma\delta}) \cdot y_{ij}^{\gamma\delta} \quad (2)$$

where γ and δ specify sublattices α or β, $\omega^{\gamma\delta}$ the number of pairs specified by superscripts in a unit cell, and $r^{\gamma\delta}$ and $y_{ij}^{\gamma\delta}$ are, respectively, the interatomic distance and the pair probability of finding an i–j pair located on a γ–δ sublattice. For the $L1_0$ ordered phase, $\omega^{\alpha\alpha} = \omega^{\beta\beta} = 1$ and $\omega^{\alpha\beta} = 4$, while the distinction between sublattices diminishes for a disordered phase and the first summation is replaced by the multiplication of 6. Among three kinds of $r^{\gamma\delta}$, i.e. $r^{\alpha\alpha}$, $r^{\alpha\beta}$ and $r^{\beta\beta}$, it is noted that $r^{\alpha\alpha} = r^{\beta\beta} \neq r^{\alpha\beta}$ and the tetragonality $\theta(=c/a)$ is equivalent to $\sqrt{2(r^{\alpha\beta})^2 - (r^{\alpha\alpha})^2}/r^{\alpha\alpha}$. Without the distinction of sublattices for a disordered phase, θ should become unity.

At the ground state of the $L1_0$ ordered phase, the atomic configuration is perfectly ordered. Hence, $y_{\mathrm{FeFe}}^{\alpha\alpha} = y_{\mathrm{PdPd}}^{\beta\beta} = y_{\mathrm{FePd}}^{\alpha\beta} = 1$ and all other pair probabilities vanish. Together with the L-J potential given by Eq. (1), and by substituting these values into Eq. (2), followed by minimization of the internal energy through

$$\frac{\partial E_{L1_0}}{\partial r^{\alpha\alpha}} = \frac{\partial E_{L1_0}}{\partial r^{\alpha\beta}} = 0 \quad (3)$$

one can obtain the ground-state energies as well as the equilibrium value of θ. The result is shown in Fig. 3 by a solid line. One confirms that the equilibrium θ corresponding to a minimum energy deviates from unity, implying that a cubic structure is energetically degenerating and an introduced freedom of two distinctive lattice constants lifts the degeneracy leading to a lower energy state. It is stressed that this point has been overlooked in most previous calculations involving $L1_0$ phase equilibria. The effects on resultant phase boundaries are discussed in the latter part of this report. However, reproducing the experimental θ value mentioned above has not been successful. In fact, θ corresponding to the minimum energy is 1.044, which is an overestimate by ~0.08. The disagreement may be ascribed either to the employed experimental data or to the procedure for determining the L-J potential. This point should be clarified in the future.

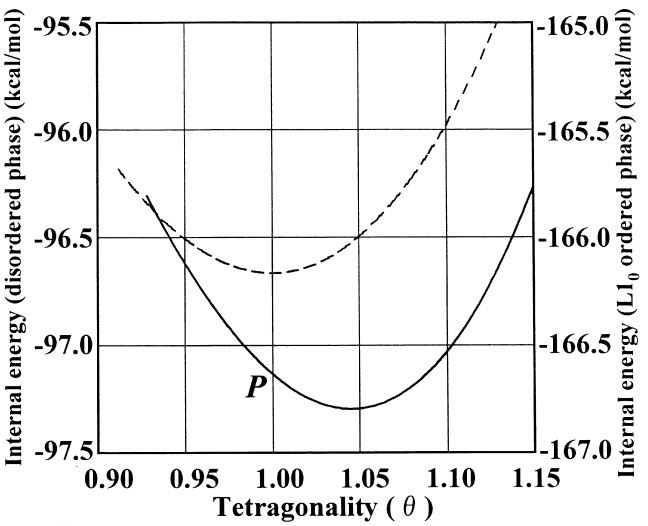

Fig. 3. Ground-state energies for a perfect $L1_0$ ordered phase and a completely random disordered phase as a function of tetragonality $\theta(=c/a)$.

It is important to examine if a minimum of internal energy of disordered solid solution can be attained at $\theta = 1$, since no tetragonality is involved in a disordered phase. Then, the internal energy of a hypothetical random solid solution is calculated by substituting $y_{ij} = 0.25$, which is the pair probability for a complete random arrangement at 50at%. The result is shown in Fig. 3 by a broken curve, and confirms that the minimum is attained exactly at $\theta = 1$. The higher internal energy of a disordered solution indicates that a disordered phase cannot be realized at the ground state.

The CVM has been recognized as one of the most powerful tools in calculating a phase equilibrium. The common practice for a fcc-based system is the employment of the tetrahedron approximation [15] in which a nearest neighbor tetrahedron is employed as a basic cluster and the atomic correlations on subclusters contained in the tetrahedron cluster are explicitly considered in the entropy formula. In the present study, the resultant expression of the entropy formula is modified for a tetragonal distortion and is given as,

$$S_{L1_0} = k_B \Bigg[\sum_{\gamma\delta} \omega^{\gamma\delta} \sum_{i,j} L(y_{ij}^{\gamma\delta}) - \frac{5}{2} \sum_{i} (L(x_i^{\alpha}) + L(x_i^{\beta})) - 2 \sum_{i,j,k,l} L(w_{ijkl}^{\alpha\alpha\beta\beta}) + 1 \Bigg] \quad (4)$$

where x and w represent point and tetrahedron cluster probabilities, respectively, of finding the atomic configuration specified by subscripts on the sublattice indicated by superscripts. For a disordered phase, a conventional tetrahedron approximation given by the following formula is employed,

$$S_{dis} = k_B \Bigg[6 \sum_{i,j} L(y_{ij}) - 5 \sum_{i} L(x_i) - 2 \sum_{i,j,k,l} L(w_{ijkl}) + 1 \Bigg] \quad (5)$$

Note that both formulae are defined per lattice point.

The free energy of the $L1_0$ phase is given as the sum of the internal energy defined in Eq. (2) and the entropy in Eq. (4), and is symbolically written as

$$F(\{e_{ij}(r^{\gamma\delta})\},\{x_i^{\gamma}\},\{y_{ij}^{\gamma\delta}\},\{w_{ijkl}^{\alpha\alpha\beta\beta}\}) = E(\{e_{ij}(r^{\gamma\delta})\},\{y_{ij}^{\gamma\delta}\}) - T \cdot S(\{x_{ij}^{\gamma}\},\{y_{ij}^{\gamma\delta}\},\{w_{ijkl}^{\alpha\alpha\beta\beta}\}) = F(\{r^{\gamma\delta}\},\{x_i^{\gamma}\},\{y_{ij}^{\gamma\delta}\},\{w_{ijkl}^{\alpha\alpha\beta\beta}\}) \quad (6)$$

The minimization of the above free energy is performed with respect to $\{r^{\gamma\delta}\}$ and $\{w_{ijkl}^{\alpha\alpha\beta\beta}\}$ under normalization and geometrical conditions that interrelate $\{w_{ijkl}^{\alpha\alpha\beta\beta}\}$ with $\{x_i^{\gamma}\}$ and $\{y_{ij}^{\gamma\delta}\}$,

$$\left.\frac{\partial F}{\partial\{w_{ijkl}^{\alpha\alpha\beta\beta}\}}\right|_{T,r^{\alpha\alpha},r^{\alpha\beta}} = \left.\frac{\partial F}{\partial r^{\alpha\alpha}}\right|_{T,r^{\alpha\beta},\{w_{ijkl}^{\alpha\alpha\beta\beta}\}} = \left.\frac{\partial F}{\partial r^{\alpha\beta}}\right|_{T,r^{\alpha\alpha},\{w_{ijkl}^{\alpha\alpha\beta\beta}\}} = 0 \quad (7)$$

The superscript can be omitted for a disordered phase. It is noted that the minimization through Eq. (7) provides not only the equilibrium free energy but also the optimized set of cluster probabilities at the equilibrium state, which help one to obtain detailed information of atomic configurations on a discrete lattice.

3. Results and discussion

3.1. Phase diagram

The phase diagram is demonstrated in Fig. 4. The broken lines indicate the phase boundaries without tetragonal distortion while the solid lines are the phase boundaries with tetragonal distortion. The experimental boundaries are shown by dotted lines [13]. This figure confirms that, with the introduction of tetragonal distortion, the experimental transition temperature is well reproduced. This can be explained in the following manner.

When the tetragonal distortion is neglected, the internal energy of the $L1_0$ phase is evaluated at $\theta = 1$, which corresponds to P in Fig. 3. Whereas, by introducing the tetragonality, the internal energy is lowered, down to the bottom of the curve, and the $L1_0$ phase is further stabilized. In fact, the introduction of the tetragonal distortion provides the system with the freedom of two different atomic distances. The increased freedom allows the system to shift to a lower energy state.

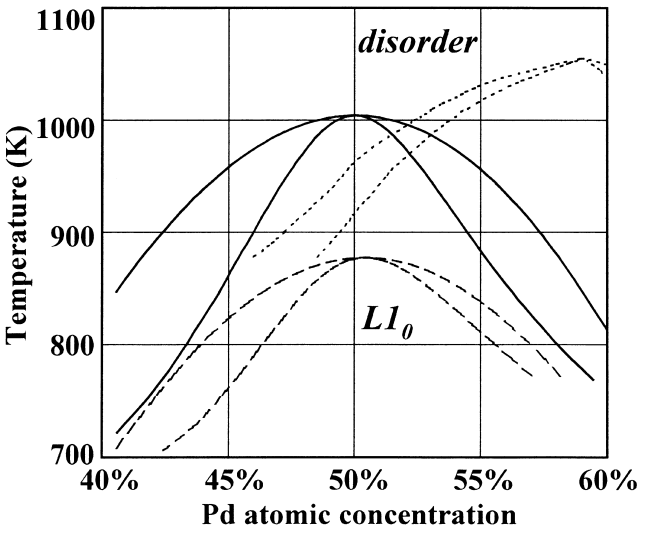

Fig. 4. Phase boundaries for disorder–$L1_0$ transition for an Fe–Pd system. The solid and broken lines, respectively, indicate the phase boundaries with and without tetragonal distortion, while the dotted lines are the experimental ones.

However, the present scheme is not fully successful in shifting the entire boundary to the Pd-rich side. The discrepancy of the congruent compositions between the present results and experimental result is still an unsettled problem. It is anticipated that the proper reproduction of tetragonality, θ, and shift of the congruent composition are interconnected problems, and that the modifications of L-J potentials are indispensable. Together with the multi-body interactions, more systematic investigation, including magnetism, is necessary for the ground state. We point out that this point should be well clarified with the cluster expansion [16,17] of total energies obtained by the electronic structure calculations.

3.2. Magnetic interaction

In most transition metal alloys, a magnetic transition characterized by Curie temperature takes place at a temperature below the phase boundary. For a system in which the Curie temperature is located close to the phase boundary, one may anticipate that the magnetic transition would affect the order–disorder transition temperature. In the present calculations, attempted for the Fe–Pd alloy, only the chemical interactions within the L-J potential were considered. In view of the relatively high Curie temperature reported for this system [13], it is desirable to incorporate the magnetic interaction into the calculation. However, derivation of the magnetic interaction energy and full calculation of a phase diagram with chemical and magnetic interactions are quite difficult tasks. Therefore, in the following, we attempt a preliminary analysis.

Within the spirit of the CVM, the up and down spins can be dealt with as different chemical species. Then, for a binary alloy system A–B, where species A is magnetic and B is non-magnetic, the system can be regarded virtually as a A_u–A_d–B ternary system where the subscripts u and d represent up and down spins, respectively. Both the internal energy and entropy formulae given by Eqs. (2) and (4) are readily extended to a ternary system by running the subscripts i, j, k and l from 1 to 3 instead of from 1 to 2 for a binary system. The numerical minimization of the resultant free energy formula becomes a bit more complicated but the essential procedure is the same as in a binary system.

In the present preliminary calculations, instead of employing the L-J potential $\{e_{ij}(r)\}$, r-independent pair-wise interaction energies $\{e_{ij}\}$ are introduced. The employed energy values are tabulated in Table 3. As will be described, the interaction energy, ϵ, between up and down spins of species A is a variable and other variables are fixed. When ϵ is unity, there is no distinction for species A_u and A_d, and the system is reduced to the original binary system. For this case, the $L1_0$–disorder transition temperature at the 1:1 stoichiometric composition is determined to be $k_B \cdot T/v_2 = 1.893$, where v_2 is the nearest neighbor

Table 3
Pair-wise interaction energies[a]

	A_u	A_d	B
A_u	1	ε	−1
A_d	ε	1	−1
B	−1	−1	1

[a] The interaction energy, ε, between up and down spins is a variable.

effective pair interaction energy, defined as $v_2 = (\epsilon_{AA} + \epsilon_{BB})/2 - \epsilon_{AB}$.

In Fig. 5, the three kinds of representative spin configurations studied in the present investigation are shown. Both the top and bottom (001) planes are occupied by A atoms for which three different spin configurations are indicated, while the intermediate (001) plane is occupied by non-magnetic B atoms. It is noted that $\uparrow\downarrow$ in configuration 3 indicates that a lattice point is occupied by up and down spins with equal probability. When one focuses on a single (001) plane of A atoms, configurations 1, 2 and 3 represent anti-ferromagnetic, ferro-magnetic and paramagnetic configurations, respectively.

Fig. 6 demonstrates the ground-state energies for these three configurations as a function of ϵ. Solid, broken and dotted lines indicate para, ferro and anti-ferro configurations, respectively. These are calculated based on Eq. (2) by neglecting the dependence on r. One can see that all three configurations degenerate energetically at $\epsilon = 1$ and, above (below) this value, the ferromagnetic (anti-ferromagnetic) configuration becomes most stable. The deviation of ϵ from unity is regarded as the contribution of the magnetic interaction.

The present calculations for finite temperatures were attempted at a fixed composition of 1:1 stoichiometry. In order to simulate the Fe–Pd system, we investigated the case of $\epsilon = 1.01$ for which the additional magnetic interaction energy is regarded as 0.01 and the ground state is ferromagnetism. The temperature dependences of two kinds of pair cluster probabilities at 1:1 stoichiometry are shown in Fig. 7. The solid line is the sum of and $y_{A_uA_u}$ and $y_{A_dA_d}$ while the broken line indicates $y_{A_uA_d}$. One sees that

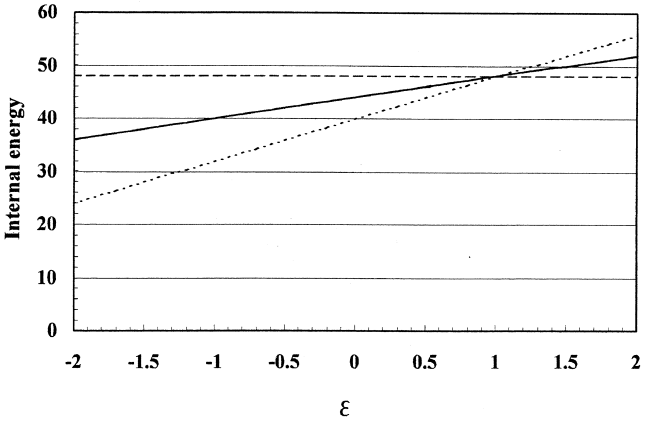

Fig. 6. Ground-state energies for the three spin configurations shown in Fig. 5 as a function of pair-wise interaction energy, ϵ, between up and down spins. Solid, broken and dotted lines correspond to para-, ferro and anti-ferro configurations, respectively.

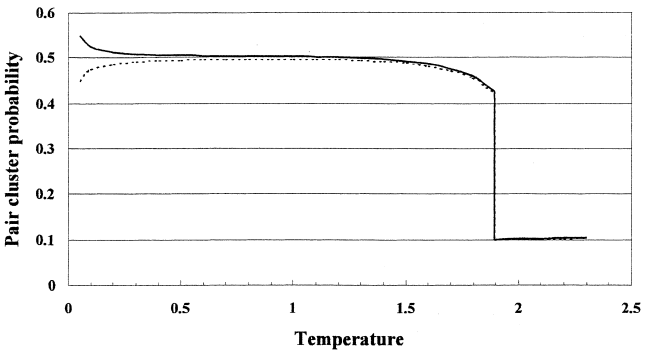

Fig. 7. Temperature dependences of nearest-neighbor pair probabilities for like spin (up–up + down–down) and unlike spin (up–down) pairs. The former is indicated by solid and the latter by dotted lines. The temperature axis is normalized with respect to the nearest neighbor effective pair interaction energy.

probabilities of like spin pairs ($y_{A_uA_u} + y_{A_dA_d}$) are much larger than those of unlike spin pairs ($y_{A_uA_d}$) in the low temperature region, indicating that the ferromagnetic configuration is predominant. Two curves merge with increas-

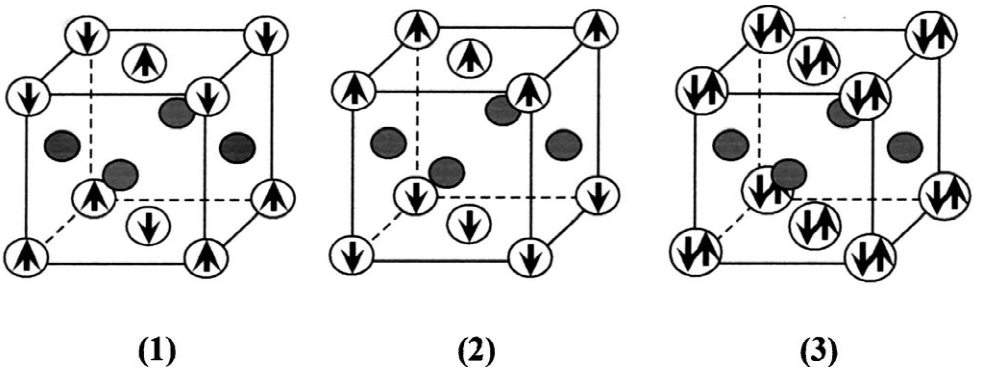

Fig. 5. Three representative spin configurations on an α-sublattice with an $L1_0$ ordered structure. (1), (2) and (3) correspond to anti-ferro, ferro and paramagnetic configurations, respectively.

ing temperature, suggesting that a ferro→para-magnetic transition is taking place with second-order character. At around a temperature of 1.4, the sum of these pair probabilities starts to deviate from unity, indicating the substitution of $B(A)$ atoms into the $\alpha(\beta)$ sublattice, which is the initiation of *chemical* $L1_0$-disorder transition. From the behavior of the curve, one can confirm that the transition is quite sharp, and is first-order in nature, and that the transition temperature was 1.896. Then, the present calculations indicate that the additional ferromagnetic interaction raises the $L1_0$-disorder transition temperature. This is because the additional magnetic interaction virtually increases the pair-wise interaction energy between species A, which destabilizes an A–A bonding. Therefore, an A–B pair is relatively stabilized against like pairs, resulting in the retardation of the disordering reaction, $A\text{–}B \rightarrow A\text{–}A + B\text{–}B$. The systematic investigation with larger values of ϵ is now under way, which is expected to provide the magnitude of the magnetic interaction energy necessary to fill the gap in the transition temperatures shown in Fig. 4.

As mentioned above, the additional magnetic interaction energy in the present study is 0.01 with respect to the chemical interaction energy of 1.0. These values, however, do not have solid physical bases. Together with more rigorous calculations with multi-body interactions, the precise evaluation of magnetic interaction energy remains a subject for future study. In addition, it is worth pointing out that neglecting the local lattice relaxation effects has been known to destabilize the disordered phase [18]. The ferro-magnetic interaction and the local lattice relaxation, therefore, induce counter-effects. We believe that the subtle balance of these two effects is a key to the further improvement of the theoretical calculation of phase boundaries.

References

[1] M. Igarashi, S. Muneki, in: M. Koiwa et al. (Eds.), Proc. Intn'l Conf. Solid–Solid Trans. '99 (JIMIC-3), The Japan Institute of Metals, 1999, p. 1156.
[2] R. Kikuchi, Phys. Rev. 81 (1951) 988.
[3] J. Sanchez, J.R. Barefoot, R.N. Jarrett, J.K. Tien, Acta Metal. 32 (1984) 1519.
[4] C.-S. Oh, T. Mohri, D.N. Lee, Mater. Trans. JIM 35 (1994) 445.
[5] T. Mohri, I. Yamagishi, T. Suzuki, C.-S. Oh, D.N. Lee, M. Yashima, M. Yoshimura, C. Ohno, Z. Metallkunde, Bd. 86 (1995) 353.
[6] R. Oshima, H. Tokoro, Bull. JPN. Inst. of Metals 62 (1998) 317, (in Japanese).
[7] Ye.V. Pal′guev, A.A. Kuranov, P.N. Syutkin, F.A. Sidorenko, Phys. Metals Metallography 42 (1976) 46, translated from Fizika Metallv, Metallovedenie 1.
[8] In: Selected Values of the Thermodynamic Properties of the Elements, ASM (1973).
[9] In: NBS Technical Note, Selected Values of Chemical Thermodynamic Properties (1969) 270.
[10] In: Landolt-Bornstein III/14-a (1988), Structure Data of Elements and Intermetallic Phases (1988).
[11] P. Villars, L.D. Calvert (Eds.), 2nd Edition, Pearson's Handbook of Crystallographic Data for Intermetallic Phases, Vol. 3, 1991.
[12] R.H. Schroder, N. Schmitz-Pranghe, R. Kohlhaas, Z. Metallkunde, Bd. 63 (1972) H.12.
[13] In: Landolt-Bornstein IV/5-e (1995). Phase Equilibria, Crystallographic and Thermodynamic Data of Binary Alloys (1995).
[14] T. Horiuchi, H. Uzawa, M. Igarashi, F. Abe, T. Mohri, in preparation.
[15] R. Kikuchi, J. Chem. Phys. 60 (1974) 1071.
[16] J.M. Sanchez, F. Ducastelle, D. Gratias, Physica (Utrecht) 128A (1984) 334.
[17] J.W.D. Connolly, A.R. Williams, Phys. Rev. B27 (1983) 5169.
[18] T. Horiuchi, S. Takizawa, T. Suzuki, T. Mohri, Metall. Mat. Trans. A 26A (1995) 11.